Ultracold Gas of Dipolar NaCs Ground State Molecules

Ian Stevenson, Aden Z. Lam, Niccolò Bigagli, Claire Warner, Weijun Yuan, Siwei Zhang, and Sebastian Will

Phys. Rev. Lett. **130**, 113002 — Published 16 March 2023

DOI: 10.1103/PhysRevLett.130.113002

Ultracold Gas of Dipolar NaCs Ground State Molecules

Ian Stevenson, Aden Z. Lam, Niccolò Bigagli, Claire Warner, Weijun Yuan, Siwei Zhang, and Sebastian Will*
[1]*Department of Physics, Columbia University, New York, New York 10027, USA*
(Dated: January 17, 2023)

We report on the creation of bosonic NaCs molecules in their absolute rovibrational ground state via stimulated Raman adiabatic passage. We create ultracold gases with up to 22,000 dipolar NaCs molecules at a temperature of 300(50) nK and a peak density of $1.0(4)\times10^{12}$ cm^{-3}. We demonstrate comprehensive quantum state control by preparing the molecules in a specific electronic, vibrational, rotational, and hyperfine state. We measure the ground state ac polarizability at 1064 nm along with the two-body loss rate, which we find to be universal. Employing the tunability and strength of the permanent electric dipole moment of NaCs, we induce dipole moments of up to 2.6 D at a DC electric field of 2.1(2) kV/cm and demonstrate strong microwave coupling between the two lowest rotational states with a Rabi frequency of $2\pi\times45$ MHz. A large electric dipole moment, accessible at relatively small electric fields, makes ultracold gases of NaCs molecules well-suited for the exploration of strongly interacting phases of dipolar quantum matter.

Ultracold dipolar molecules [1, 2] are a unique platform for the investigation of new areas in molecular and many-body quantum physics [3, 4]. Studies with dipolar ground state molecules are enabling advances in quantum chemistry [5–8] and have exciting prospects for quantum simulation [9, 10], quantum computing [11–13] and the investigation of novel quantum phases [14, 15]. Their electric dipole moment gives rise to tunable long-range interactions that can be controlled via external electric [7, 16, 17] or microwave [18–20] fields. Many applications of dipolar molecules will require quantum degenerate molecular gases.

Molecular ensembles with the highest phase-space densities have been created via assembly of ultracold molecules from ultracold gases of atoms [21–23]; first, weakly bound Feshbach molecules [24] are created and then transferred to their rovibrational ground state via two-photon transfer. This approach has been previously employed to create ultracold gases of KRb [22], RbCs [25, 26], NaK [27–30], NaRb [31], NaLi [32], and single NaCs [33] ground state molecules. Recently, for the fermionic molecules KRb [34] and NaK [35], direct creation of degenerate molecular Fermi gases has been demonstrated. Also, collisional shielding [36–38] and microwave shielding [39] have been demonstrated to suppress two-body losses and enable evaporative cooling. For ultracold gases of bosonic ground state molecules, collisional shielding, evaporative cooling, and the formation of a Bose-Einstein condensate are outstanding goals.

In this Letter, we report on the production of ultracold gases of strongly dipolar NaCs molecules in their rovibrational ground state. Using stimulated Raman adiabatic passage (STIRAP) [40], we create up to 22,000 ground state molecules in a specific hyperfine state at a temperature of 300(50) nK. Under these conditions, we estimate a phase-space density of about 0.01 and determine a two-body loss rate of $7(3)\times10^{-10}$ cm^{3}s^{-1}, which we find to be universal. In addition, we expose the molecular gases to electric fields of up to 2.1(2) kV/cm and observe Stark shifts of the ground state that correspond to an induced dipole moment of up to 2.6 D, which is significantly larger than the highest induced dipole moment in previous work [7].

NaCs stands out due to its large dipole moment of $d = 4.75(20)$ D [41, 42] in the rovibrational ground state. As a result, the effective range of dipole-dipole interactions, $a_\mathrm{d} = md^2/(8\pi\varepsilon_0\hbar^2)$, can reach tens of micrometers, an order of magnitude larger than for NaK and two orders of magnitude larger than for KRb (m denotes the molecular mass). The large dipole moment also promises that shielding techniques, which generally scale proportional to higher powers of d [43–45], will be highly effective. Bulk gases of strongly dipolar NaCs molecules, which we create in this work, will allow for the exploration of new phases of dipolar quantum matter, facilitate the loading of extended optical lattice and tweezer arrays, and promise new avenues for quantum simulation and quantum computing.

The experiment starts with an ultracold gas of 4×10^4 NaCs Feshbach molecules that are associated from ultracold gases of Na and Cs via a magnetic field ramp across the Feshbach resonance at 864.12(5) G [46, 47]. Details of the molecule preparation can be found in Refs. [47, 48]. Na and Cs are in their lowest hyperfine state $|f,m_f\rangle = |1,1\rangle$ and $|3,3\rangle$, respectively. The Feshbach molecules are prepared at a magnetic field of 863.84(1) G with a binding energy of about 500 kHz; their molecular state has about 25% singlet and 75% triplet character, with the dominant bound-state contributions being $|S=1,m_S=0,m_{I_\mathrm{Na}}=3/2,m_{I_\mathrm{Cs}}=5/2\rangle$ and $|S=1,m_S=1,m_{I_\mathrm{Na}}=3/2,m_{I_\mathrm{Cs}}=3/2\rangle$. Here, S is the quantum number of the electronic spin, and m_S its projection on the quantization axis; m_{I_Na} (m_{I_Cs}) is the projection of the Na (Cs) nuclear spin. The molecular gas is held in a crossed optical dipole trap operating at 1064 nm; the trap frequencies are $\omega = \{\omega_x,\omega_y,\omega_z\} = 2\pi\times\{30(3),60(5),130(5)\}$ Hz. For detection, the molecules are dissociated into free atoms via a reverse magnetic field ramp and imaged at low field.

We have developed a coherent two-photon scheme that transfers ultracold gases of NaCs Feshbach molecules to the rovibrational ground state via an electronically excited state that has mixed singlet and triplet spin character (see Fig. 1). For the laser that couples the Feshbach state $|F\rangle$ to the excited state $|E\rangle$ (laser 1), we use a titanium-sapphire laser that operates near 916 nm; its polarization is parallel with respect to

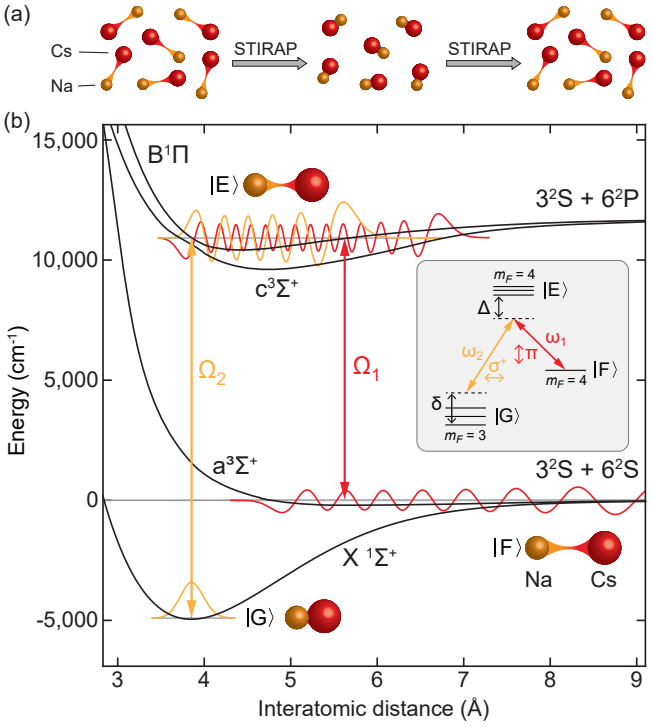

FIG. 1. Two-photon pathway to the rovibrational ground state of NaCs. (a) An ultracold bulk gas of weakly bound NaCs Feshbach molecules is transferred to the ground state via STIRAP. Prior to detection, STIRAP is applied in reverse. (b) Molecular potentials of NaCs as relevant for transfer to the rovibrational ground state $X^1\Sigma^+ |v = 0,\ J = 0,\ m_J = 0\rangle$. Here, J denotes the total angular momentum and m_J its projection on the quantization axis. Ω_1 and Ω_2 denote the Rabi frequencies of the Raman lasers. The inset shows the relevant sublevels, including the m_F quantum numbers that are accessible with the given laser polarizations. Δ and δ denote the one- and two-photon detuning from the excited state and the ground state, respectively. Arrows indicate light polarizations relative to the quantization axis set by the vertical magnetic field.

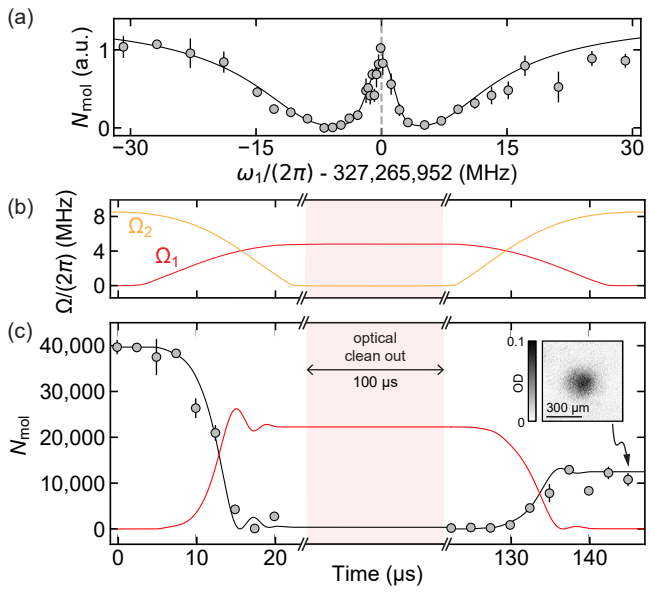

FIG. 2. Creation of NaCs ground state molecules. (a) Coupling to the rovibrational ground state via $B^1\Pi |v = 10\rangle$ is observed in two-photon dark resonance spectroscopy. The solid line is a fit to a master equation model yielding Rabi frequencies $\Omega_1/2\pi = 0.6(1)$ MHz and $\Omega_2/2\pi = 8.8(5)$ MHz. (b) STIRAP is realized via a ramp of laser intensities, giving rise to a dynamic change of the Rabi frequencies Ω_1 (red) and Ω_2 (orange) as shown. (c) Evolution of the number of Feshbach molecules (circles) during the STIRAP sequence. The black solid line shows a fit of the Feshbach molecule number to a master equation model that also yields the number of molecules in the ground state (red solid line). The inset shows a background-free absorption image of about 1.2×10^4 Feshbach molecules after a STIRAP round trip and 17 ms time of flight. For this data, $\Omega_1/2\pi = 4.5$ MHz, $\Omega_2/2\pi = 8.4$ MHz, $\Delta/2\pi = 90$ MHz, and $\delta/2\pi = 0$ MHz.

the quantization axis (defined by the vertical magnetic field). For the laser that couples the excited state $|E\rangle$ to the rovibrational ground state $|G\rangle$ (laser 2), we use an external cavity diode laser that operates near 632 nm; its polarization is orthogonal with respect to the quantization axis. In order to establish phase coherence between the lasers on the relevant time scale (less than 1 ms), we stabilize their absolute frequencies to the kilohertz-level by locking them to an optical cavity made from ultralow expansion glass via the Pound-Drever-Hall technique.

As a bridge to the ground state, we use an electronically excited state in the $c^3\Sigma^+ \sim B^1\Pi$ complex as shown in Fig. 1(b). Due to strong spin-orbit coupling in NaCs [49, 50], many vibrational states have strongly mixed singlet and triplet spin character. However, we have found that states of the $c^3\Sigma^+ \sim B^1\Pi$ complex have unconventionally broad linewidths, which is unsuitable for resonant or near-resonant STIRAP. For example, in recent work, Cairncross et al. [33] have demonstrated ground state transfer of an individually trapped NaCs molecule via far off-resonant Raman-Rabi transfer using the $c^3\Sigma^+ |v = 26, J = 1\rangle$ state (v denotes the vibrational state). We found this state to have a linewidth of $2\pi \times 51(5)$ MHz, which is significantly broader than realistically achievable Rabi frequencies. In this work, we have identified the $B^1\Pi |v = 10,\ J = 1,\ m_J = 1\rangle$ as a suitable intermediate state. Additional spectroscopic details of the $c^3\Sigma^+ \sim B^1\Pi$ complex will be discussed in Ref. [51].

We experimentally locate the ground state [52, 53] via dark resonance spectroscopy, as shown in Fig. 2 (a). Dark resonance spectroscopy also allows us to measure the excited state linewidth Γ and Rabi couplings Ω_1 and Ω_2 by fitting the data with a three-state model [54, 55]. Combining the results of measurements at different laser powers [56], we obtain $\Gamma/2\pi = 15(3)$ MHz for the $B^1\Pi |v = 10,\ J = 1,\ m_J = 1\rangle$ state. For the laser powers available in our setup, we can reach Rabi frequencies of up to $\Omega_1^{\max}/2\pi \approx 12$ MHz and $\Omega_2^{\max}/2\pi \approx 25$ MHz, which is on the order of the excited state linewidth. To realize STIRAP, we dynamically change the Rabi frequencies Ω_1 and Ω_2 [Fig. 2 (b)], which transfers the molecules to the ground state and back, while

the system remains in the dark state whose population is proportional to $\cos[\theta(t)]|F\rangle - \sin[\theta(t)]|G\rangle$, where $\theta(t) = \tan^{-1}(\Omega_1/\Omega_2)$ [40]. Between forward and reverse STIRAP, a 100 μs-pulse of resonant laser light removes remaining Na and Cs atoms and Feshbach molecules [56]. This increases the detected molecule number by a factor of three compared to a slower removal scheme based on a magnetic field gradient, which we employed in earlier work [47].

Figure 2 (c) shows transfer to the ground state by monitoring the Feshbach molecule population during the STIRAP sequence. We have found robust conditions for 20 μs long pulses, shown in Fig. 2 (b) and used for all data in this paper, and a one-photon detuning of $\Delta/2\pi = -90$ MHz. Starting with 4×10^4 Feshbach molecules, we detect 1.2×10^4 Feshbach molecules after the STIRAP round trip. This corresponds to a one-way transfer efficiency of 55(3) %. About 2.2×10^4 ground-state molecules are created with a peak density of $1.0(4) \times 10^{12}$ cm^{-3} and a phase-space density of 0.01.

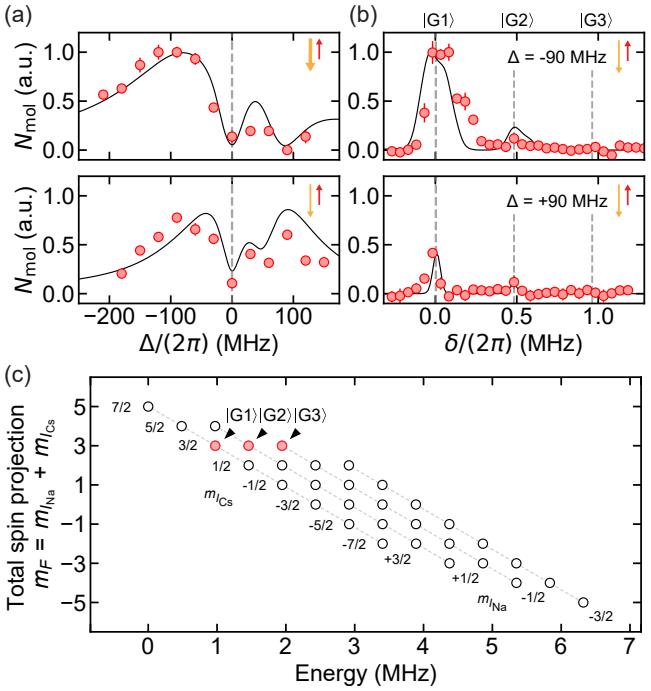

FIG. 3. Controlling the hyperfine state of NaCs ground state molecules. (a) Dependence of transfer efficiency on the one-photon detuning Δ, while staying on resonance with the ground state ($\delta = 0$). Top (bottom) panel corresponds to $\Omega_1/2\pi = 4.5$ MHz and $\Omega_2/2\pi = 8.4$ MHz ($\Omega_1/2\pi = 4.5$ MHz and $\Omega_2/2\pi = 4.5$ MHz). (b) Accessible hyperfine states for $\Delta/2\pi = -90$ MHz (top) and $\Delta/2\pi = +90$ MHz (bottom) with $\Omega_1 = \Omega_2 = 2\pi \times 4.5$ MHz. Solid lines in (a) and (b) are calculated from a master equation model to be reported in Ref. [51]. (c) Energies of all $(2I_{Na}+1)(2I_{Cs}+1) = 32$ hyperfine ground states at a magnetic field of 863.84 G. The hyperfine structure is in the Paschen-Back regime, dominated by the nuclear Zeeman effect, while scalar spin-spin interactions are weak ($c_4 = 3941.8$ Hz [57]). The initial Feshbach state has $m_F = 4$. Hyperfine states that can be addressed in our coupling scheme are shown as red dots.

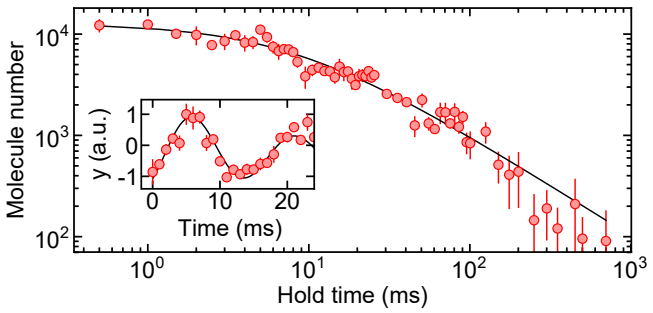

FIG. 4. Lifetime of NaCs in the rovibrational ground state measured for an initial peak density of $5(3)\times10^{11}$ cm^{-3} and temperature of 300(50) nK. The solid line shows a fit to a two-body decay model. Data points correspond to the average of three experimental runs. The inset shows a trap frequency measurement of ground state molecules oscillating along the y-axis. From this we determine a ratio for the ac polarizabilities of the ground state molecules and Cs atoms of 0.77(1) in the optical dipole trap at 1064 nm.

In Fig. 3 (a), we show the transfer efficiency as a function of one-photon detuning. We find that our system significantly deviates from the behavior of a canonical three-level STIRAP model, where most efficient transfer is expected on resonance ($\Delta = 0$) [58]. Instead, our one-photon detuning spectra show nearly vanishing transfer efficiency on resonance for a pulse duration of 20 μs; in addition, they are highly asymmetric and tend to favor negative one-photon detuning. We attribute this behavior to unresolved hyperfine structure in the excited state [28, 30, 59]; laser 1 with π-polarized light leaves $m_F = 4$ of the initial Feshbach state unchanged and can in principle couple to three hyperfine states fulfilling $m_F = 4$ [see inset of Fig. 1 (b)]. Taking into account the multi-level structure, we have developed a numerical model [56], which accurately captures the behavior of our system (solid lines in Fig. 3). The model suggests that the observed STIRAP efficiency is largely limited by the multi-level structure and not by laser noise.

In Figure 3 (b) we demonstrate controlled transfer into a well-defined hyperfine level. To this end, we have measured distinct STIRAP resonances in the rovibrational ground state by varying the two-photon detuning δ for two different one-photon detunings Δ. While laser 1 leaves $m_F = 4$ unchanged, laser 2 couples to the ground state via horizontal polarization, corresponding to $(\sigma^+ + \sigma^-)/\sqrt{2}$ light, which, in principle, gives access to $m_F = 3$ and 5. However, experimentally we see dominant coupling into $|G1\rangle$ and weak coupling to $|G2\rangle$ with $m_F = 3$; coupling to the absolute hyperfine ground state with $m_F = 5$ is not observed and likely suppressed due to the absence of an $|m_{I_{Na}} = 3/2, m_{I_{Cs}} = 7/2\rangle$ admixture in $|E\rangle$. The observed splitting between $|G1\rangle$ and $|G2\rangle$ of 483(1) kHz [56] is consistent with the prediction of the ground state hyperfine structure, shown in Fig. 3 (c).

Equipped with the ability to create spin-polarized ultracold gases of NaCs ground state molecules, we study their collisional properties. Figure 4 shows a lifetime measurement for an ensemble with a peak density of $n_0 = 5(3) \times 10^{11}$ cm^{-3}

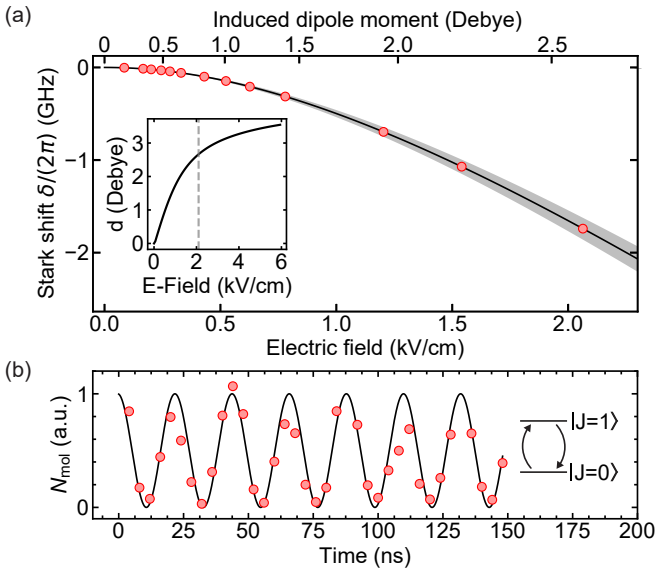

FIG. 5. Strong dipole moment of NaCs molecules. (a) NaCs molecules in a homogeneous electric field. The Stark shift of the ground state is measured via dark resonance spectroscopy (red circles). Error bars are smaller than the point size. The solid line corresponds to the calculation of the expected Stark shift based on the known permanent dipole moment d [41] and the rotational constant of the ground state. The gray shading reflects the uncertainty in the dipole moment. The Stark shift is used to calibrate the electric field strength. The inset shows the induced dipole moment d versus dc electric field; the dashed rectangle indicates the dipole moments of up to 2.6 Debye reached in this work. (b) Fast Rabi oscillations between rotational states of NaCs. The population in the rotational ground state ($J = 0$) is measured as a function of time. The optical dipole trap is switched off during the microwave pulse. The solid line is a sinusoidal fit yielding a Rabi frequency of 45.4(3) MHz. The microwave frequency is about 3.471 GHz. Further details on rotational spectra of NaCs will be reported elsewhere [70].

and a temperature of 300(50) nK. In order to determine the molecular density, we measure the molecular trap frequencies. By comparing the molecular trap frequencies to those of the Cs atoms [56, 60], as shown in the inset to Fig. 4, we determine the polarizability of the molecules at 1064 nm to be $h \times 41(1)$ Hz/(W/cm^2). This compares reasonably well to Ref. [61] which predicts $h \times 35$ Hz/(W/cm^2). The lifetime data closely follows a two-body loss model with a decay rate of $\Gamma_{2B}^{\rm exp} = 7(3) \times 10^{-10}$ cm^3 s^{-1} and a characteristic decay time of $1/(\Gamma_{2B}\bar{n}) = 10(1)$ ms, where $\bar{n}$ is the average density [62]. Our measurement agrees well with the predicted theoretical two-body collision rate, $\Gamma_{2B}^{\rm th} = 8 \times 10^{-10}$cm^3 s^{-1} [43]. This suggests that NaCs, similar to other bialkali species, exhibits unity loss at short range, although direct two-body loss is energetically forbidden [63]. The exact nature of the two-body loss process is an open question [17, 64–68] and future studies of NaCs will provide a valuable data point in this fast-evolving field [69].

Strong dipole-dipole interactions between NaCs molecules can be induced by aligning their electric dipole moments in the laboratory frame using a homogeneous electric field. In Figure 5 (a) we demonstrate the effect of a dc electric field on the ground state by monitoring its Stark shift, which is directly related to the magnitude of the induced dipole moment. Homogeneous electric fields with up to 2.1(2) kV/cm are generated at the location of the molecules using indium tin oxide coated glass electrodes, mounted outside of the ultrahigh vacuum chamber. First, we confirm via one-photon spectroscopy that the Stark shift of the excited state is negligible even for the strongest fields. Then, we determine the Stark shift of the ground state via dark resonance spectroscopy. For the largest field, we observe a Stark shift of 1.8 GHz, which corresponds to an induced dipole moment of 2.6 Debye.

In addition, we demonstrate strong microwave coupling between the rotational ground ($J = 0$) and first excited state ($J = 1$) in NaCs. The coupling scales linearly in the dipole moment, $dE_{\rm ac}$, where $E_{\rm ac}$ is the electric-field strength of the microwave. We observe fast Rabi oscillations with a frequency of up to $2\pi \times 45$ MHz, as shown in Fig. 5 (b), indicating further enhanced coupling compared to recent demonstrations with NaK [39] and CaF [71]. For quantum information applications [11], the fast Rabi oscillations can enable rotational single-qubit gates on a time-scale of few nanoseconds, surpassing or rivaling existing quantum information platforms.

Recently, it has been shown that resonant collisional shielding [37, 38] and microwave shielding [39, 71] can enable effective evaporative cooling. For NaCs, resonant shielding is predicted to lead to an extremely favorable ratio of elastic to inelastic collisions of 10^6 [38, 44]. This requires accessing a Förster resonance in the $|J, m_J\rangle = |1, 0\rangle$ state, located at an electric field of 2.5 kV/cm [44], which can be reached with minor technical upgrades. Microwave shielding [45, 72] is also expected to be highly effective thanks to weak hyperfine interactions and strong microwave coupling. This makes NaCs a promising candidate for evaporative cooling towards a Bose-Einstein condensate of dipolar ground state molecules, which is an important prerequisite for applications of dipolar molecules in quantum simulation [4].

In conclusion, we have created an ultracold gas of 22,000 NaCs ground state molecules at 300(50) nK. Using STIRAP, we have prepared the molecules with full control over their electronic, vibrational, rotational, and hyperfine state. Demonstrating the tunability and strength of the electric dipole moment, we have exposed the molecular ensembles to electric fields that induce a dipole moment of up to 2.6 Debye. These conditions, combined with prospects for effective repulsive shielding protocols, make NaCs an exceptional candidate for the demonstration of evaporative cooling of bosonic ground state molecules, Bose-Einstein condensation, the exploration of new phases of matter, and applications in quantum simulation and quantum information.

We thank Eberhard Tiemann for providing a coupled-channel calculation for the Feshbach state, Kang-Kuen Ni and her group for fruitful discussions, and Tarik Yefsah for helpful comments on the manuscript. We also thank Emily Bellingham for experimental assistance. This work was supported

by an NSF CAREER Award (Award No. 1848466), an ONR DURIP Award (Award No. N00014-21-1-2721) and a Lenfest Junior Faculty Development Grant from Columbia University. C.W. acknowledges support from the Natural Sciences and Engineering Research Council of Canada (NSERC) and the Chien-Shiung Wu Family Foundation. W.Y. acknowledges support from the Croucher Foundation. I.S. was supported by the Ernest Kempton Adams Fund. S.W. acknowledges additional support from the Alfred P. Sloan Foundation.

* sebastian.will@columbia.edu

[1] L. D. Carr, D. DeMille, R. V. Krems, and J. Ye, New J. Phys. **11**, 055049 (2009).
[2] S. A. Moses, J. P. Covey, M. T. Miecnikowski, D. S. Jin, and J. Ye, Nature Phys. **13**, 13 (2017).
[3] T. Lahaye, C. Menotti, L. Santos, M. Lewenstein, and T. Pfau, Rep. Prog. Phys. **72**, 126401 (2009).
[4] M. A. Baranov, M. Dalmonte, G. Pupillo, and P. Zoller, Chem. Rev. **112**, 5012 (2012).
[5] R. V. Krems, Phys. Chem. Chem. Phys. **10**, 4079 (2008).
[6] G. Quemener and P. S. Julienne, Chem. Rev. **112**, 4949 (2012).
[7] M. Guo, X. Ye, J. He, M. L. González-Martínez, R. Vexiau, G. Quéméner, and D. Wang, Phys. Rev. X **8**, 041044 (2018).
[8] M.-G. Hu, Y. Liu, D. D. Grimes, Y.-W. Lin, A. H. Gheorghe, R. Vexiau, N. Bouloufa-Maafa, O. Dulieu, T. Rosenband, and K.-K. Ni, Science **366**, 1111 (2019).
[9] A. Micheli, G. Brennen, and P. Zoller, Nature Phys. **2**, 341 (2006).
[10] E. Altman, K. R. Brown, G. Carleo, L. D. Carr, E. Demler, C. Chin, B. DeMarco, S. E. Economou, M. A. Eriksson, K.-M. C. Fu, M. Greiner, K. R. Hazzard, R. G. Hulet, A. J. Kollár, B. L. Lev, M. D. Lukin, R. Ma, X. Mi, S. Misra, C. Monroe, K. Murch, Z. Nazario, K.-K. Ni, A. C. Potter, P. Roushan, M. Saffman, M. Schleier-Smith, I. Siddiqi, R. Simmonds, M. Singh, I. Spielman, K. Temme, D. S. Weiss, J. Vučković, V. Vuletić, J. Ye, and M. Zwierlein, PRX Quantum **2**, 017003 (2021).
[11] D. DeMille, Phys. Rev. Lett. **88**, 067901 (2002).
[12] A. André, D. DeMille, J. M. Doyle, M. D. Lukin, S. E. Maxwell, P. Rabl, R. J. Schoelkopf, and P. Zoller, Nat. Phys. **2**, 636 (2006).
[13] R. Sawant, J. A. Blackmore, P. D. Gregory, J. Mur-Petit, D. Jaksch, J. Aldegunde, J. M. Hutson, M. R. Tarbutt, and S. L. Cornish, New J. Phys. **22**, 013027 (2020).
[14] H. P. Büchler, E. Demler, M. Lukin, A. Micheli, N. Prokof'ev, G. Pupillo, and P. Zoller, Phys. Rev. Lett. **98**, 060404 (2007).
[15] B. Capogrosso-Sansone, C. Trefzger, M. Lewenstein, P. Zoller, and G. Pupillo, Phys. Rev. Lett. **104**, 125301 (2010).
[16] M. De Miranda, A. Chotia, B. Neyenhuis, D. Wang, G. Quéméner, S. Ospelkaus, J. Bohn, J. Ye, and D. Jin, Nature Phys. **7**, 502 (2011).
[17] R. Bause, A. Schindewolf, R. Tao, M. Duda, X.-Y. Chen, G. Quéméner, T. Karman, A. Christianen, I. Bloch, and X.-Y. Luo, Phys. Rev. Research **3**, 033013 (2021).
[18] B. Yan, S. A. Moses, B. Gadway, J. P. Covey, K. R. Hazzard, A. M. Rey, D. S. Jin, and J. Ye, Nature **501**, 521 (2013).
[19] S. A. Will, J. W. Park, Z. Z. Yan, H. Loh, and M. W. Zwierlein, Phys. Rev. Lett. **116**, 225306 (2016).
[20] Z. Z. Yan, J. W. Park, Y. Ni, H. Loh, S. Will, T. Karman, and M. Zwierlein, Phys. Rev. Lett. **125**, 063401 (2020).
[21] W. Stwalley, Eur. Phys. J. D **31**, 221 (2004).
[22] K.-K. Ni, S. Ospelkaus, M. De Miranda, A. Pe'Er, B. Neyenhuis, J. Zirbel, S. Kotochigova, P. Julienne, D. Jin, and J. Ye, Science **322**, 231 (2008).
[23] J. G. Danzl, M. J. Mark, E. Haller, M. Gustavsson, R. Hart, J. Aldegunde, J. M. Hutson, and H.-C. Nägerl, Nat. Phys. **6**, 265 (2010).
[24] C. Chin, R. Grimm, P. Julienne, and E. Tiesinga, Rev. Mod. Phys. **82**, 1225 (2010).
[25] T. Takekoshi, L. Reichsöllner, A. Schindewolf, J. M. Hutson, C. R. Le Sueur, O. Dulieu, F. Ferlaino, R. Grimm, and H.-C. Nägerl, Phys. Rev. Lett. **113**, 205301 (2014).
[26] P. K. Molony, P. D. Gregory, Z. Ji, B. Lu, M. P. Köppinger, C. R. Le Sueur, C. L. Blackley, J. M. Hutson, and S. L. Cornish, Phys. Rev. Lett. **113**, 255301 (2014).
[27] J. W. Park, S. A. Will, and M. W. Zwierlein, Phys. Rev. Lett. **114**, 205302 (2015).
[28] F. Seeßelberg, N. Buchheim, Z.-K. Lu, T. Schneider, X.-Y. Luo, E. Tiemann, I. Bloch, and C. Gohle, Phys. Rev. A **97**, 013405 (2018).
[29] L. Liu, D.-C. Zhang, H. Yang, Y.-X. Liu, J. Nan, J. Rui, B. Zhao, and J.-W. Pan, Phys. Rev. Lett. **122**, 253201 (2019).
[30] K. K. Voges, P. Gersema, M. Meyer zum Alten Borgloh, T. A. Schulze, T. Hartmann, A. Zenesini, and S. Ospelkaus, Phys. Rev. Lett. **125**, 083401 (2020).
[31] M. Guo, B. Zhu, B. Lu, X. Ye, F. Wang, R. Vexiau, N. Bouloufa-Maafa, G. Quéméner, O. Dulieu, and D. Wang, Phys. Rev. Lett. **116**, 205303 (2016).
[32] T. M. Rvachov, H. Son, A. T. Sommer, S. Ebadi, J. J. Park, M. W. Zwierlein, W. Ketterle, and A. O. Jamison, Phys. Rev. Lett. **119**, 143001 (2017).
[33] W. B. Cairncross, J. T. Zhang, L. R. B. Picard, Y. Yu, K. Wang, and K.-K. Ni, Phys. Rev. Lett. **126**, 123402 (2021).
[34] L. De Marco, G. Valtolina, K. Matsuda, W. G. Tobias, J. P. Covey, and J. Ye, Science **363**, 853 (2019).
[35] M. Duda, X.-Y. Chen, A. Schindewolf, R. Bause, J. von Milczewski, R. Schmidt, I. Bloch, and X.-Y. Luo, arXiv:2111.04301 (2021).
[36] G. Valtolina, K. Matsuda, W. G. Tobias, J.-R. Li, L. De Marco, and J. Ye, Nature **588**, 239 (2020).
[37] K. Matsuda, L. De Marco, J.-R. Li, W. G. Tobias, G. Valtolina, G. Quéméner, and J. Ye, Science **370**, 1324 (2020).
[38] J.-R. Li, W. G. Tobias, K. Matsuda, C. Miller, G. Valtolina, L. De Marco, R. R. Wang, L. Lassablière, G. Quéméner, J. L. Bohn, and J. Ye, Nat. Phys. **17**, 1144 (2021).
[39] A. Schindewolf, R. Bause, X.-Y. Chen, M. Duda, T. Karman, I. Bloch, and X.-Y. Luo, arXiv:2201.05143 (2022).
[40] N. V. Vitanov, A. A. Rangelov, B. W. Shore, and K. Bergmann, Rev. Mod. Phys. **89**, 015006 (2017).
[41] P. J. Dagdigian and L. Wharton, J. Chem. Phys. **57**, 1487 (1972).
[42] M. Aymar and O. Dulieu, J. Chem. Phys. **122**, 204302 (2005).
[43] P. S. Julienne, T. M. Hanna, and Z. Idziaszek, Phys. Chem. Chem. Phys. **13**, 19114 (2011).
[44] M. L. González-Martínez, J. L. Bohn, and G. Quéméner, Phys. Rev. A **96**, 032718 (2017).
[45] L. Lassablière and G. Quéméner, Phys. Rev. Lett. **121**, 163402 (2018).
[46] J. T. Zhang, Y. Yu, W. B. Cairncross, K. Wang, L. R. Picard, J. D. Hood, Y.-W. Lin, J. M. Hutson, and K.-K. Ni, Physical Review Letters **124**, 253401 (2020).
[47] A. Z. Lam, N. Bigagli, C. Warner, W. Yuan, S. Zhang, E. Tiemann, I. Stevenson, and S. Will, Phys. Rev. Research **4**,

L022019 (2022).
[48] C. Warner, A. Z. Lam, N. Bigagli, H. C. Liu, I. Stevenson, and S. Will, Phys. Rev. A **104**, 033302 (2021).
[49] M. Korek, S. Bleik, and A.-R. Allouche, J. Chem. Phys. **126**, 124313 (2007).
[50] J. Zaharova, M. Tamanis, R. Ferber, A. Drozdova, E. Pazyuk, and A. Stolyarov, Phys. Rev. A **79**, 012508 (2009).
[51] C. Warner, N. Bigagli, A. Z. Lam, W. Yuan, S. Zhang, E. Tiemann, I. Stevenson, and S. Will, (in preparation).
[52] O. Docenko, M. Tamanis, R. Ferber, A. Pashov, H. Knöckel, and E. Tiemann, Eur. Phys. J. D **31**, 205 (2004).
[53] P. Zabawa, A. Wakim, M. Haruza, and N. Bigelow, Phys. Rev. A **84**, 061401 (2011).
[54] M. Fleischhauer, A. Imamoglu, and J. P. Marangos, Rev. Mod. Phys. **77**, 633 (2005).
[55] R. Bause, A. Kamijo, X.-Y. Chen, M. Duda, A. Schindewolf, I. Bloch, and X.-Y. Luo, Phys. Rev. A **104**, 043321 (2021).
[56] See Supplemental Material at X for details on the calibration of Rabi couplings, the optical clean out of remaining atoms, and the optimal conditions for STIRAP transfer.
[57] J. Aldegunde and J. M. Hutson, Phys. Rev. A **96**, 042506 (2017).
[58] M. O. Scully and M. S. Zubairy, "Quantum Optics," (1999).
[59] N. Vitanov and S. Stenholm, Physical Review A **60**, 3820 (1999).
[60] C. Ravensbergen, V. Corre, E. Soave, M. Kreyer, S. Tzanova, E. Kirilov, and R. Grimm, Physical review letters **120**, 223001 (2018).
[61] R. Vexiau, D. Borsalino, M. Lepers, A. Orbán, M. Aymar, O. Dulieu, and N. Bouloufa-Maafa, International Reviews in Physical Chemistry **36**, 709 (2017).
[62] The fit function for two-body decay has the form $N(t) = N_0/(1+\Gamma_{2B}\bar{n}t)$, where N_0 is the initial molecule number. The average density $\bar{n}$ of a thermal gas in a harmonic trap is given by $\bar{n} = n_0/2^{3/2}$, where n_0 is the peak density.
[63] P. S. Żuchowski and J. M. Hutson, Phys. Rev. A **81**, 060703 (2010).
[64] M. Mayle, B. P. Ruzic, and J. L. Bohn, Phys. Rev. A **85**, 062712 (2012).
[65] M. Mayle, G. Quéméner, B. P. Ruzic, and J. L. Bohn, Physical Review A **87**, 012709 (2013).
[66] P. D. Gregory, J. A. Blackmore, S. L. Bromley, and S. L. Cornish, Phys. Rev. Lett. **124**, 163402 (2020).
[67] Y. Liu, M.-G. Hu, M. A. Nichols, D. D. Grimes, T. Karman, H. Guo, and K.-K. Ni, Nature Physics **16**, 1132 (2020).
[68] P. Gersema, K. K. Voges, M. M. zum Alten Borgloh, L. Koch, T. Hartmann, A. Zenesini, S. Ospelkaus, J. Lin, J. He, and D. Wang, Phys. Rev. letters **127**, 163401 (2021).
[69] R. Bause, A. Christianen, A. Schindewolf, I. Bloch, and X.-Y. Luo, arXiv preprint arXiv:2211.10223 (2022).
[70] N. Bigagli, C. Warner, A. Z. Lam, W. Yuan, S. Zhang, I. Stevenson, and S. Will, (in preparation).
[71] L. Anderegg, S. Burchesky, Y. Bao, S. S. Yu, T. Karman, E. Chae, K.-K. Ni, W. Ketterle, and J. M. Doyle, Science **373**, 779 (2021).
[72] T. Karman and J. M. Hutson, Phys. Rev. Lett. **121**, 163401 (2018).